Unliganded gating of acetylcholine receptor channels

Prasad Purohit and Anthony Auerbach[1]

Department of Physiology and Biophysics, University at Buffalo, State University of New York, Buffalo, NY 14214

Edited by Richard W. Aldrich, University of Texas, Austin, TX, and approved November 14, 2008 (received for review September 18, 2008)

We estimated the unliganded opening and closing rate constants of neuromuscular acetylcholine receptor-channels (AChRs) having mutations that increased the gating equilibrium constant. For some mutant combinations, spontaneous openings occurred in clusters. For 25 different constructs, the unliganded gating equilibrium constant (E_0) was correlated with the product of the predicted fold-increase in the diliganded gating equilibrium constant caused by each mutation alone. We estimate that (*i*) E_0 for mouse, wild-type $\alpha_2\beta\delta\varepsilon$ AChRs is $\approx 1.15 \times 10^{-7}$; (*ii*) unliganded AChRs open for ≈80 μs, once every ≈15 min; (*iii*) the affinity for ACh of the O(pen) conformation is ≈10 nM, or ≈15,600 times greater than for the C(losed) conformation; (*iv*) the ACh-monoliganded gating equilibrium constant is $\approx 1.7 \times 10^{-3}$; (*v*) the C→O isomerization reduces substantially ACh dissociation, but only slightly increases association; and (*vi*) ACh provides only ≈0.9 k_BT more binding energy per site than carbamylcholine but ≈3.1 k_BT more than choline, mainly because of a low O conformation affinity. Most mutations of binding site residue αW149 increase E_0. We estimate that the mutation αW149F reduces the ACh affinity of C only by 13-fold, but of O by 190-fold. Rate–equilibrium free-energy relationships for different regions of the protein show similar slopes (Φ values) for un- vs. diliganded gating, which suggests that the conformational pathway of the gating structural change is fundamentally the same with and without agonists. Agonist binding is a perturbation that (like most mutations) changes the energy, but not the mechanism, of the gating conformational change.

allosteric | protein | synapse | kinetics | spontaneous

The acetylcholine receptor (AChR) is a large, 5-subunit ion channel (1–4) that can adopt stable conformations called **C**(losed) and **O**(pen). These two structures are distinguished by two essential properties: the **C** conformation has a lower affinity for agonists and a lower ionic conductance compared with **O**. In the absence of agonists, the probability that a wild-type (WT) AChR adopts the **O** shape is exceedingly low, and there is almost no current flow at the synapse. When a high concentration of agonist is present, for example after the release of an ACh-filled vesicle from the motor nerve terminal, two binding sites located in the extracellular domain of the protein are occupied by transmitter molecules, and the entire pentamer transiently adopts the **O** shape, both rapidly (≈20 μs) and with a high probability (≈0.95).

The allosteric control for the overall **C**↔ **O** gating isomerization, which in our experiments includes both the affinity change and the conductance change, is the presence of a ligand at each transmitter binding site (TBS). Ligand binding and channel gating are coupled energetically [supporting information (SI) Fig. S1]. For small agonist molecules, the two TBSs are approximately equivalent and independent in the **C** conformation (mouse AChRs) (5); assuming that this also holds for the **O** conformation, and without any external energy,

$$E_2/E_0 = (K_d/J_d)^2 \quad [1]$$

E_2 is the diliganded gating equilibrium constant, E_0 is the unliganded gating equilibrium constant, K_d is the equilibrium dissociation constant of **C**, and J_d is the equilibrium dissociation constant of **O**. E_2 and K_d have been measured experimentally in WT AChRs (≈30 and ≈150 μM, respectively, adult mouse and human AChRs activated by ACh, 23 °C, −100 mV) (6–8), but it has proven to be difficult to measure E_0 and J_d because both are small so un- and monoliganded states are rarely visited.

Unliganded gating of mouse AChRs has been studied for both WT (9, 10) and many different mutants that exhibit an increased frequency of spontaneous openings (11–17). Jackson (10) estimated that upon agonist binding, WT AChRs expressed in muscle cells increase their opening frequency and lifetime by factors of 1.4×10^7 and 5, respectively. Grosman (13) examined various gain-of-function AChR mutants and concluded that the position of the transition state along the reaction coordinate is different for unliganded vs. diliganded AChR gating.

In these pioneering studies, E_0 was small, and unliganded openings were infrequent. The primary goals of our experiments were to study AChRs having large gain-of-function mutations to measure directly E_0 for WT AChRs and to investigate further whether unliganded and diliganded AChR gating occur by the same reaction mechanism.

Results

Estimation of E_0. AChR structure and the locations of the mutated residues are shown in Fig. S2.The effect of each mutation on E_2 is given in Table S1. In WT AChRs, unliganded openings are both rare and brief, but their frequency increases in receptors with mutations that increase E_2, presumably because of a parallel increase in E_0 (Fig. 1*A*). When E_0 is sufficiently large, unliganded openings occur in clusters (each arising from a single AChR), with the intervals between clusters reflecting sojourns in desensitized states. The long-lived intervals associated with these sojourns are similar in unliganded and diliganded AChRs (Fig. 1*B*) (18), indicating that the presence of agonists at the transmitter binding sites is not required for AChRs to enter states that are associated with desensitization. Also, E_0 is similar in different ionic strength extracellular solutions, which suggests that ions are not acting as agonists (Table S2 and Figs. S3 and S4*a*).

The durations of intervals within unliganded clusters often exhibit multiple closed and open components (10, 13); and to estimate E_0, we must identify which of these components arise from the unliganded, **C**↔ **O** gating isomerization. A single, intracluster open-and-shut component was predominant for the AChR constructs that we examined for unliganded gating (Fig. 2 and Fig. S3).

To estimate E_0 for WT AChRs, we made three assumptions: (*i*) The inverse lifetimes of the predominant shut (open) component of the interval duration histograms reflects the opening (closing) rate constant of unliganded **C**↔ **O** gating. (*ii*) The fold-increases in E_2 for each mutation arise exclusively from a parallel increase in E_0 (there was no effect of mutations on the affinity ratio,

Author contributions: P.P. and A.A. designed research; P.P. performed research; P.P. analyzed data; and A.A. wrote the paper.

The authors declare no conflict of interest.

This article is a PNAS Direct Submission.

[1]To whom correspondence should be addressed at: 309C Cary Hall, South Campus, University at Buffalo, State University of New York, Buffalo, NY 14214. E-mail: auerbach@buffalo.edu.

This article contains supporting information online at www.pnas.org/cgi/content/full/0809272106/DCSupplemental.

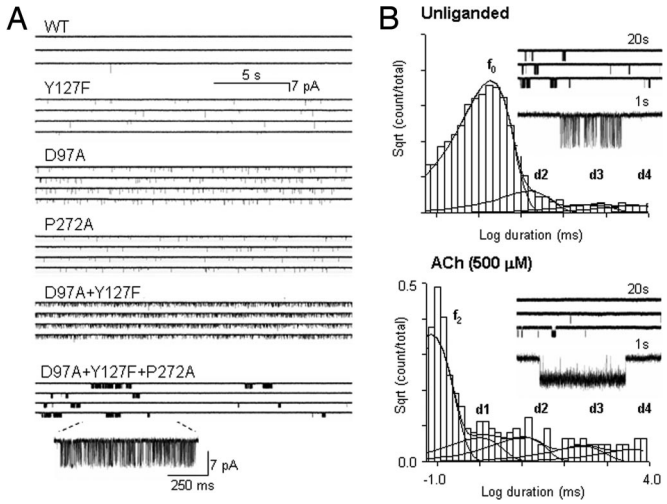

Fig. 1. Example single-channel currents of unliganded AChRs. (*A*) The frequency of unliganded activity is higher in gain-of-function mutants (AChRs having higher diliganded gating equilibrium constants; Table S1). In constructs with multiple mutations, for instance αD97A/αY127F/αP272A, spontaneous openings occur in clusters, with the intervals between clusters reflecting sojourns in desensitized states. (*B*) AChR desensitization is approximately the same with and without agonists present at the transmitter binding sites. Nonconducting interval duration histograms are shown for αD97A/αY127F/αP272A AChRs (*Upper*, unliganded; *Lower*, activated by 500 μM ACh). The desensitized components are marked as d_1, d_2, d_3, and d_4; b_0 and b_2 mark the component arising from unliganded and diliganded channel opening. Component d_1 is not visible in unliganded currents because it overlaps with the gating component (f_0). The d_2–d_4 time constants and relative frequencies are similar in unliganded (13, 372, and 4,169 ms; frequency ratio 7.8, 1.1, 1.0) vs. diliganded (8.9, 224, and 3,354 ms; frequency ratio 3.7, 1.4, 1.0) gating (see also ref. 18).

K_d/J_d). (*iii*) The effects of the mutations on E_0 are independent energetically, so that AChRs with multiple mutations exhibit a fold-increase in E_0 (relative to the WT value) that is the product of the fold-increases in E_2 for each mutation.

For 25 different cluster-producing mutant combinations, the observed value of E_0 for each mutant combination was correlated with the expected fold-increase in E_2, calculated as the product of the fold-increases for each individual mutation (Fig. 3). We estimated E_0^{WT} by dividing the observed E_0 value by the expected E_2 fold-increase, for each construct (Table S2). The average of this ratio was $E_0^{WT} = 1.15 \pm 0.28 \times 10^{-7}$ (mean ± SE).

We draw two conclusions from the relatively small variance of the E_0^{WT} estimate. First, all of the above assumptions are, approximately, sustained. If a point mutation altered the affinity ratio or if there was energetic coupling between point mutations, then the observed E_0 for that particular combination would not be expected to fall on the correlation line. The correlation in Fig. 3 also implies that the difference in the energetic consequence of each mutation to the ground states ($\Delta\Delta G^{\mathbf{C-O}}$) is similar in diliganded and unliganded AChRs. Second, for the mutations we examined, all that counts with regard to E_0 is $\Delta\Delta G^{\mathbf{C-O}}$, not the location or Φ value (see below) of the perturbation.

Despite the high degree of correlation and the low variance, there is additional uncertainty in the estimate for E_0^{WT}. Only a handful of mutants were used, and any error in the E_2 for each construct (including the WT) will propagate to the E_0^{WT} estimate. Also, small degrees of energetic coupling between different mutant side chains, or small effects of the mutations on the affinity ratio, might also bias the E_0^{WT} estimate.

There are conflicting reports that the mutation αE45R either decreases (8) or increases (19) E_2. In two mutant backgrounds, αE45R increased E_0 (Table S2).

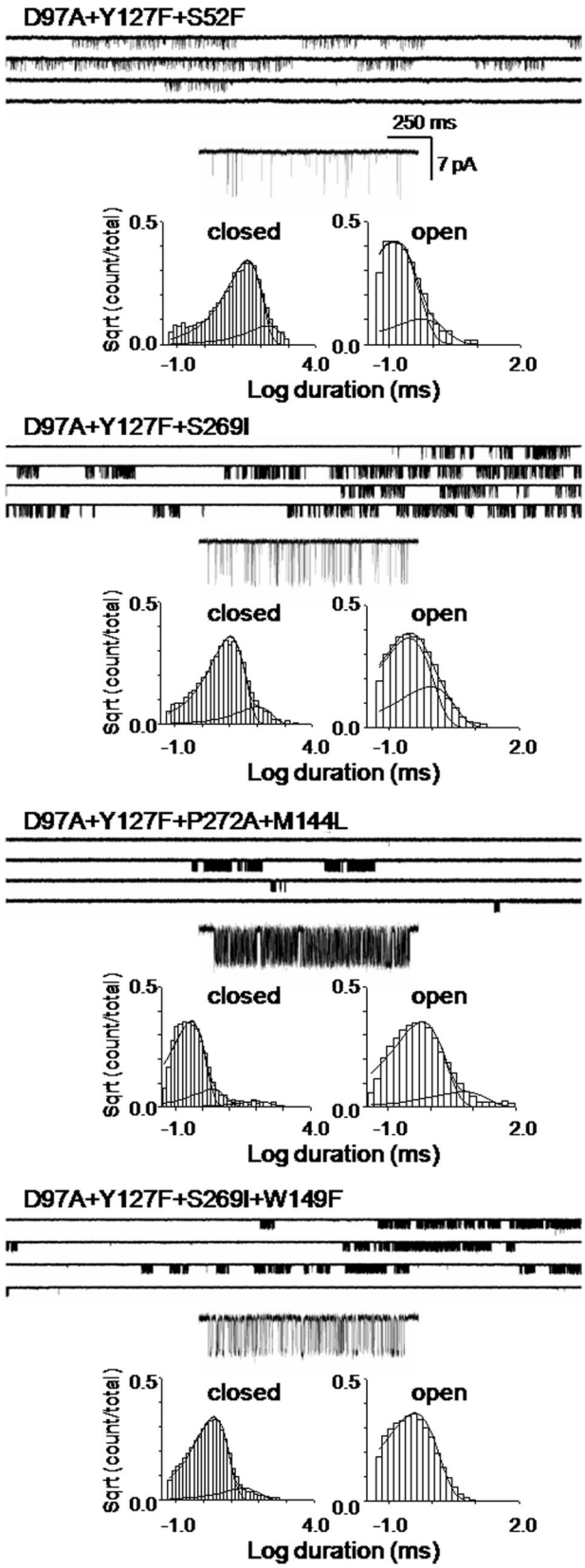

Fig. 2. Example unliganded currents from AChRs with multiple mutations. (*Upper*) Clusters of openings. (*Lower*) Corresponding intracluster interval duration histograms. Note that the αW149F mutation has a higher frequency of spontaneous opening than the background α(D97A/Y127F/S269I). The predominant component from each distribution was taken to reflect unliganded, **C**↔ **O** gating. More examples are shown in Fig. S3.

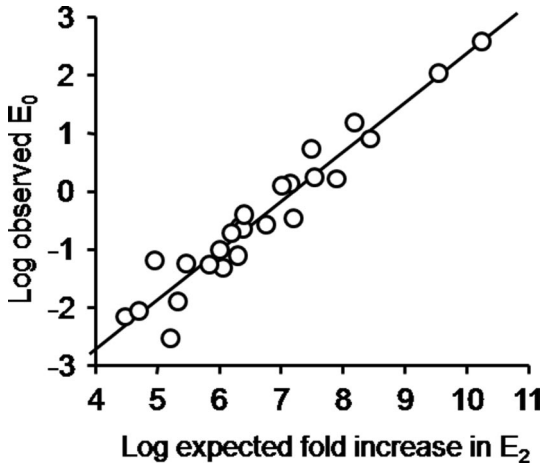

Fig. 3. The observed E_0 is correlated with the predicted, aggregate effect of the mutations on E_2. E_0 was estimated from the predominant components of the intracluster interval durations for AChRs having a combination of gain-of-function mutations. The expected fold-increase effect on E_2 was the product of the fold-changes in E_2 measured for each point mutant in each combination. The high degree of correlation ($r = 0.96$; 25 different combinations; Table S2) suggests that the increase in E_2 for each point mutant arose from a parallel change in E_0 and that the energetic consequences of the mutations were independent. We estimated E_0^{WT} by dividing the observed E_0 value by the expected E_2 fold-increase, for each construct (Table S2). The average of the ratio 9observed E_0 value/expected E_2 fold-increase0 for all constructs is an estimate of $E_0^{WT} = 1.15 \times 10^{-7}$.

Unliganded Gating Reaction Mechanism. Is the **C**↔ **O** gating reaction mechanism the same with and without exogenous ligands at the transmitter binding sites? Certain evidence suggests that the answer to this question is "yes." The selectivity and conductance of unliganded single-channel currents are the same as for diliganded currents (9) (Fig. S4*b*), which suggests that the structures of the open-channel-domain with and without ligands at the TBS are similar. Also, the observations that α-bungarotoxin blocks spontaneous openings of WT AChRs (9) (Fig. S4*c*) and that mutations of residues that decrease E_2 also decrease the frequency of unliganded openings (13) suggest that the structures and gating conformational changes at the TBS are similar in the apo- and liganded AChR. The above observation that the energetic-consequences mutations are similar in diliganded and unliganded gating also implies that the **C** and **O** and state structures are similar in the apo- and liganded AChRs.

Other evidence suggests that the answer to the question is "no." The relative extent to which a perturbation that changes E_2 does so by changing the diliganded opening (f_2) vs. closing rate constant reflects the energy (structure) of the perturbed site at the gating reaction transition state (**TS**). If the perturbation only changes f_2, then the site of the perturbation at the **TS** is deemed to be "**O**-like" in character (structure and dynamics), whereas if it only changes the closing rate constant the site is "**C**-like." The relative extent of reaction progress is given by Φ, which is the straight-line slope of a log–log plot of f_2 vs. E_2 (a rate-equilibrium free-energy relationship, or REFER) (20). Thus, Φ values are experimental measurements that illuminate the intermediate states of the **C**↔ **O** isomerization that are, in our experiments, too brief to be detected directly (21).

For diliganded gating, there is an approximately longitudinal, decreasing, and coarse-grained gradient in Φ down the long axis of the α subunit, with some exceptions (22). At the **TS**, TBS residues are mostly **O**-like (move early in the opening process) whereas pore residues are more **C**-like (move later). However, for unliganded gating, this gradient is not apparent because $\Phi \approx 1$ in many different regions of the AChR (13). For example, in diliganded gating, depolarization decreases E_2 but hardly decreases f_2 ($\Phi = 0.07$) (23); whereas for unliganded gating, the same degree of depolarization hardly increases the closing rate constant ($\Phi \approx 1$) (11). These results, with regard to mutations and the perturbation of the voltage sensor, raise the possibility that apo- and diliganded AChRs isomerize by different conformational cascade (11).

An important caveat is that REFERs are not strictly linear, and, hence, experimental Φ values can change with the magnitude of the equilibrium constant. For many chemical reactions, including AChR gating (24), there is a tendency for Φ, determined over a narrow range of E_2, to increase from 0 (**C**-like) to 1 (**O**-like) as E_2 falls from ∞ to 0 (25, 26) [a "Hammond" effect (27)]. Because the diliganded Φ measurements were carried out, typically, under conditions where $E_2 \approx 1$, and the unliganded Φ measurements were carried out under conditions where E_0 was at least a million times smaller, we tested the hypothesis that the differences in di- vs. unliganded Φ values arose from a Hammond effect.

We measured Φ values of perturbations, in different regions of the protein, by using unliganded AChRs having background mutations that increased E_0 to comparable values as in the diliganded experiments. The places tested were: the voltage sensor, L265 in the M2 (pore-lining) helix of the δ subunit, V269 in M2 of the δ subunit, V269 in M2 of the ε subunit, L279 in the M3 helices of the α subunits, W149 at the TBS of the α subunits, and the agonist itself (including none).

Fig. 4 shows that on the mutant backgrounds, all seven sites had an unliganded Φ value, and therefore a **TS** character, that was similar to that measured in diliganded experiments. This result indicates that at the overall reaction **TS**, the agonist, the TBS, αM3, δM2, εM2, and the voltage sensor all have progressed to similar degrees in the **C**→**O** channel-opening process in the apoprotein as in the fully-liganded AChR. This supports the hypothesis that the observed differences between unliganded vs. diliganded Φ values arise from Hammond effects, and it provides evidence that AChRs traverse the same **TS** ensemble with and without agonists at the binding sites.

Two panels of Fig. 4 warrant further comment. Fig. 4*G* shows that unliganded gating falls on the same line as diliganded gating (with agonists), which is to say that the character of the bound agonist at the **TS** is similar for no agonist vs. the other ligands (**O**-like). The fact that the apo condition shares the same REFER as do agonists indicates that, like most side-chain mutations, a ligand at the TBS can be treated as a straightforward perturbation of energy. Fig. 4*F* shows that many of the side-chain substitutions of TBS residue αW149 increase E_0. This is surprising because previous diliganded gating studies of this residue showed that mutations here decrease both E_2 and K_d (28) and the response EC_{50} (29). This indicates that the mechanism by which these αW149 mutations reduce E_2 is not by a parallel reduction in E_0, but rather by an increase in E_0 that is offset by an even larger reduction in the affinity ratio, K_d/J_d. Another interesting result of the αW149 experiments is that the open- and closed-interval duration histograms were monoexponential (except for desensitization), allowing for a particularly clear identification of the **C**↔ **O** gating events (Fig. 2). Perhaps some of the kinetic complexity of unliganded AChRs arises from TBS polymorphisms.

Discussion

The results indicate that for a given equilibrium constant, the overall "mechanism" of the gating conformational change [the functional properties (and, likely, structures) of the **C** and **O** end states, the position of the **TS** (Φ), the pathway(s) across the **TS**(s), and the relative timing of residue motions within the reaction] is essentially the same in unliganded and diliganded AChRs. The AChR gating reaction is remarkably robust over a

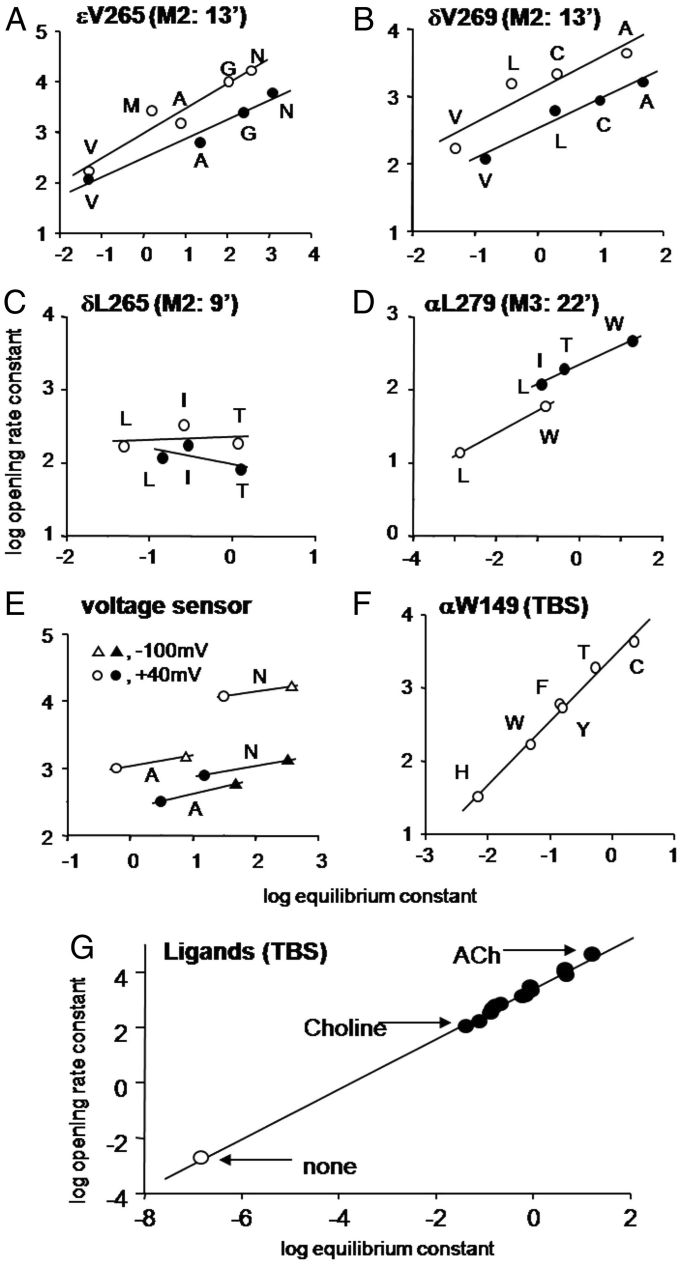

Fig. 4. The transition states for unliganded and diliganded gating are similar. The slope of the rate-equilibrium free-energy relationship, Φ, gives the fractional reaction progress of the perturbed site at the gating transition state. Φ values for 7 different positions in the AChR (Fig. S2 and Table S2) are the similar in unliganded vs. diliganded gating. For the unliganded experiments, the background construct was α(D97A+Y127F+S296I), except for αL279W, which was α(D97A+Y127F). For the diliganded experiments the background was always WT. (*A*) V265 in the M2 helix of the ε subunit (0.49 ± 0.08 vs. 0.38 ± 0.06). (*B*) V260 in the M2 helix of the δ subunit (0.49 ± 0.15 vs. 0.45 ± 0.07). (*C*) L265 in the M2 helix of the δ subunit (0.04 ± 0.22 vs. −0.22 ± 0.26). (*D*) W279 on the M3 helix of the α subunit (0.31 vs. 0.27 ± 0.02). (*E*) Voltage sensor of two different backgrounds (εV265A: 0.15 vs. 0.2; εV265N, 0.13 vs. 0.16). (*F*) W149, at the TBS of the α subunit (0.87 ± 0.03; not measured for diliganded gating, but probably ≈1). (*G*) Transmitter binding site and ligands. The agonist REFER data are from Grosman *et al.* (23). Open is unliganded, and filled is diliganded (0.91 ± 0.01). At the **TS**, the unliganded TBS has progressed to the same extent as has the ACh-occupied TBS.

$>10^8$-fold range of equilibrium constant. Agonists animate the conformational change but do not change the basic gating mechanism.

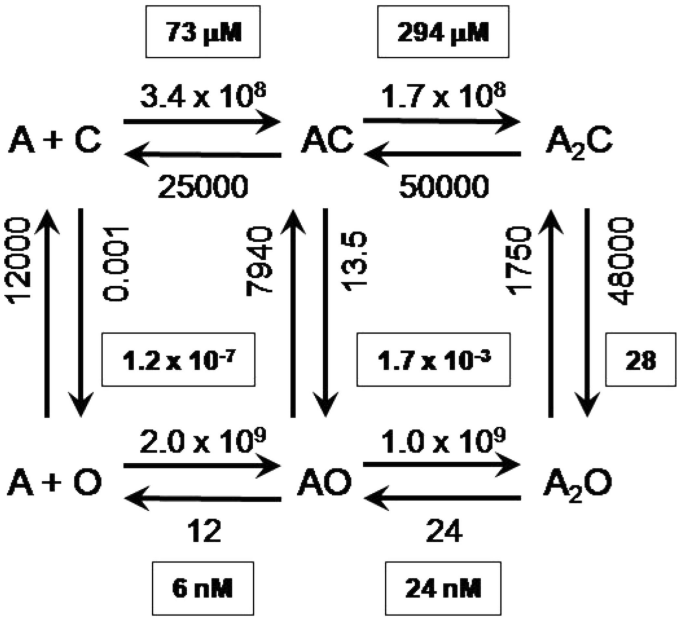

Fig. 5. Rate and equilibrium constants for ACh binding and gating of AChRs. The association rate constants are $M^{-1}\,s^{-1}$; all others are s^{-1}. The equilibrium constants are boxed (see Fig. S1). For each binding site, K_d = 146 μM and J_d = 10 nM.

The value $E_0^{WT} \approx 1.15 \times 10^{-7}$ allows the estimation of ACh binding and channel gating rate and equilibrium constants for AChRs at the neuromuscular synapse (Fig. 5).

In WT AChRs the unliganded channel-closing rate constant is ≈12,000 s^{-1} (13). From the E_0^{WT} estimate we calculate that the unliganded channel-opening rate constant is ≈0.001 s^{-1}. At synapses, each unliganded WT AChR opens for ≈80 μs, once every ≈15 min. This spontaneous activity is probably the basis for the observation that application of curare to normal muscle causes a ≈1-mV hyperpolarization (30). Slow-channel congenital myasthenia is, in some cases, caused by AChR mutations that increase E_0 (17), so in these patients the standing current will be greater. For example, with the mutation αS269I we estimate that unliganded, adult neuromuscular AChRs open spontaneously approximately once every 8 s.

We define the **C**/**O** agonist affinity ratio: $R = K_d/J_d$. In WT AChRs activated by ACh E_2 = 28, so from Eq. 1 we calculate R_{ACh} = 15,600. The affinity of the **O** conformation for ACh is this much greater than that of the **C** conformation. In terms of energy, this affinity ratio is equivalent to a stabilization of the agonist by 9.7 k_BT (5.7 kcal/mol) at each transmitter binding site, or twice this amount per AChR, in the **C**→**O** isomerization.

From Fig. S1 we calculate that the WT, ACh monoliganded gating equilibrium constant E_1 [= $(E_0{}^*R)$] is 1.7 × 10^{-3}. As shown in Fig. 4*G*, the Φ value for ligands is 0.91, so we estimate ($f_1 = f_0{}^*R_{ACh}^{0.91}$) that the opening and closing rate constants for monoliganded AChRs are ≈13.5 s^{-1} and ≈7,940 s^{-1}.

The affinity of the WT **C** conformation for ACh is K_d^{ACh} ≈150 μM, so, from the affinity ratio, we calculate that the affinity of the **O** conformation is J_d^{ACh} ≈9.7 nM. This open-state affinity is approximately the same as the desensitized-state affinity (31).

K_d is the ratio k_-/k_+, or for WT mouse AChRs and ACh, 25,000 s^{-1}/1.7 × 10^8 $M^{-1}\,s^{-1}$ (6). Assuming that the binding sites are equal and independent in both **C** and **O**, experiments show that the single-site dissociation rate constant from **O** ≈12 s^{-1} (32). Therefore, the rate constant for ACh association to the **O** conformation (j_+) is ≈1.0 × 10^9 $M^{-1}\,s^{-1}$. **C**→**O** gating entails a ≈15,600-fold increase in affinity for ACh, which arises from

a modest ≈6-fold increase in the association rate constant and a large, ≈2,100-fold decrease in the dissociation rate constant. The structural changes at the TBS during the channel-opening process serve to hold the agonist but do not much alter the ability of ACh to enter. We speculate that the movement of loop C in ligand binding reflects more the formation of a low affinity (K_d) TBS than the low-high affinity ($K_d \rightarrow J_d$) transition.

We can carry out similar analyses for different agonists. $E_2 \approx 5$ for carbamylcholine (CCh) (33) or tetramethyammonium (TMA) (28), so for these ligands $R \approx 6{,}700$ (8.8 k_BT or 5.2 kcal/mol per site). $E_2 = 0.05$ for the agonist choline (34), so $R_{Cho} \approx 660$ (6.5 k_BT or 3.8 kcal/mol per site). ACh provides only ≈0.9 k_BT (0.5 kcal/mol per site) more binding energy per site than TMA (or CCh), but ≈3.1 k_BT (1.8 kcal/mol per site) more than choline. This selectivity may have arisen through natural selection because choline is present at high concentrations at the synapse (generated by ACh hydrolysis). The "efficacy" of a ligand is more clearly and quantitatively described by its R value (net **C** vs. **O** binding energy) than by the fuzzier terms "full" or "partial" agonist. Note that for a given AChR construct, an R value ratio (ACh vs. ligand X) can be calculated without knowledge of E_0, as $\sqrt{(E_2^{ACh}/E_2^X)}$.

From the affinity ratios and the observations that $K_d^{CCh} \approx K_d^{TMA} \approx 1$ mM (28, 33) and $K_d^{Cho} \approx 4$ mM (5), we calculate $J_d^{CCh} \approx J_d^{TMA} \approx 100$ nM, and $J_d^{Cho} \approx 6$ μM. The low efficacy of choline is caused mainly by a low affinity of the **O** conformation. It will be interesting to learn what structural features of the TBS are responsible for the small R value for choline.

We now turn our attention to the TBS mutant αW149F. E_0 for this mutant is ≈3.4-fold greater than for the WT ($E_0^{\alpha W149F} \approx 3.9 \times 10^{-7}$) (Fig. 4*G*). Previous reports show that E_2 (w/ACh) for this mutant is 0.4, which is a ≈70-fold loss of function (28). We calculate: $R_{ACh}^{\alpha W149F} = 1{,}012$, which is 15.4 times smaller than in the WT. We learn that with ACh, the αW149F mutation reduces the net binding energy per site, from 9.7 k_BT (5.7 kcal/mol per site) to 6.9 k_BT (4.1 kcal/mol per site). Experiments show that $K_d^{\alpha W149F} = 1{,}920$ μM (28), so we calculate $J_d^{\alpha W149F} = 1.9$ μM. This mutation reduces the ACh affinity of **C** by 13-fold, but of **O** by 190-fold. By far, the main effect of this mutation is on the stability of the diliganded **O** conformation of the TBS.

Finally, we consider **C**↔ **O** gating as a perturbation of the A+**C**↔ A**C** binding reaction (where A represents the agonist). $\Phi_{bind} = \log(j_+/k_+)/\log(K_d/J_d)$, from the above, $\Phi_{bind} = \log(6)/\log(15{,}600) = 0.19$. By using the temporal interpretation of Φ, this fractional value (which has no error limits because it is computed from only 2 points) implies that gating occurs "late" in the binding process, but perhaps before the ligand is completely bound. In AChRs, binding and gating may not be completely separable processes. It is possible that the **C→O** isomerization starts before ACh has fully nestled into the binding pocket. Along similar lines, it is thought that S1–S2 domain motions of glutamate receptors, as viewed in X-ray structures of receptor fragments occupied by various ligands, reflect both binding and gating conformational events (35).

Materials and Methods

Mutagenesis was performed by using the QuikChange site-directed mutagenesis kit (Stratagene), and the mutations were confirmed by sequencing. The WT or mutant mouse AChR subunits were transiently expressed in human embryonic kidney 293 cells by calcium phosphate precipitation (α, β, δ, and ε; 3.5–5.5 μg total per 35-mm culture dish, in 2:1:1:1 ratio). The culture medium was washed after ≈16 h, and electrophysiological recordings were performed (22 °C) in the on-cell configuration after ≈24 h. The pipette potential was 70 mV (except where noted), corresponding to a membrane potential of ≈ −100 mV. The bath and pipette solutions were Dulbecco's PBS containing 137 mM NaCl, 0.9 mM $CaCl_2$, 2.7 mM KCl, 1.5 mM KH_2PO_4, 0.5 mM $MgCl_2$, and 8.1 mM Na_2HPO_4 (pH 7.4). The single-channel currents were filtered at 20 kHz and digitized at a sampling frequency of 50 kHz. The pipette holder and electrodes were never exposed to ligands.

Kinetic analyses were performed by using QUB software (www.qub.buffalo.edu) (see ref. 36). Because there was no agonist, there was no agonist-induced channel block. When possible, clusters of individual channel activity, flanked by ≥20-ms nonconducting periods, were selected by eye. The clusters were idealized into noise-free intervals, usually without any further filtering by using the segmental-k-means algorithm (37). The unliganded opening (f_0) and closing (b_0) rate constants were estimated from the idealized interval durations by using a maximum-interval likelihood algorithm (38) after imposing a dead time of 25 μs. The idealized, intracluster intervals were first fitted by a 2-state model (**C**↔ **O**), and additional nonconducting and conducting states were added, one at a time, connected only to the first **O** state, until the log likelihood failed to improve by >10 units. A similar approach was used to estimate the desensitized, nonconducting components, only the entire current record was idealized (no clusters, hence no truncation of the histogram), as described elsewhere (18). Φ was estimated as the linear slope of the REFER. Points in the REFER represent the mean value for the number of patches examined for each construct. The structure image was displayed by using PyMOL (DeLano Scientific).

ACKNOWLEDGMENTS. We thank Mary Merritt, Marlene Shero, and Mary Teeling for technical help. This work was supported by the National Institute of Health Grant NS23513.

1. Edelstein S, Changeux J-P (1998) Allosteric transitions of the acetylcholine receptor. *Adv Protein Chem* 51:121–184.
2. Karlin A (2002) Emerging structure of the nicotinic acetylcholine receptors. *Nat Rev Neurosci* 3:102–114.
3. Lester HA, Dibas MI, Dahan DS, Leite JF, Dougherty DA (2004) Cys-loop receptors: New twists and turns. *Trends Neurosci* 27:329–336.
4. Sine SM, Engel AG (2006) Recent advances in Cys-loop receptor structure and function. *Nature* 440:448–455.
5. Purohit Y, Grosman C (2006) Estimating binding affinities of the nicotinic receptor for low-efficacy ligands using mixtures of agonists and two-dimensional concentration–response relationships. *J Gen Physiol* 127:719–735.
6. Chakrapani S, Bailey TD, Auerbach A (2003) The role of loop 5 in acetylcholine receptor channel gating. *J Gen Physiol* 122:521–539.
7. Lape, *et al.* (2008) On the nature of partial agonism in the nicotinic receptor superfamily. *Nature* 454:722–727.
8. Lee WY, Sine SM (2005) Principal pathway coupling agonist binding to channel gating in nicotinic receptors. *Nature* 438:243–247.
9. Jackson MB (1984) Spontaneous openings of the acetylcholine receptor channel. *Proc Natl Acad Sci USA* 81:3901–3904.
10. Jackson MB (1986) Kinetics of unliganded acetylcholine receptor channel gating. *Biophys J* 49:663–672.
11. Auerbach, *et al.* (1996) Voltage dependence of mouse acetylcholine receptor gating: Different charge movements in di-, mono-, and unliganded receptors. *J Physiol* 494:155–170.
12. Engel AG, *et al.* (1996) New mutations in acetylcholine receptor subunit genes reveal heterogeneity in the slow-channel congenital myasthenic syndrome. *Hum Mol Genet* 5:1217–1227.
13. Grosman C (2003) Free-energy landscapes of ion-channel gating are malleable: Changes in the number of bound ligands are accompanied by changes in the location of the transition state in acetylcholine receptor channels. *Biochemistry* 42:14977–14987.
14. Grosman C, Auerbach A (2000) Kinetic, mechanistic, and structural aspects of unliganded gating of acetylcholine receptor channels: A single-channel study of second transmembrane segment 12′ mutants. *J Gen Physiol* 115:621–635.
15. Milone M, *et al.* (1997) Slow-channel myasthenic syndrome caused by enhanced activation, desensitization, and agonist binding affinity attributable to mutation in the M2 domain of the acetylcholine receptor α subunit. *J Neurosci* 17: 5651–5665.
16. Ohno K, *et al.* (1996) Congenital myasthenic syndrome caused by decreased agonist binding affinity due to a mutation in the acetylcholine receptor ε subunit. *Neuron* 17:157–170.
17. Zhou M, Engel AG, Auerbach A (1999) Serum choline activates mutant acetylcholine receptors that cause slow-channel congenital myasthenic syndromes. *Proc Natl Acad Sci USA* 96:10466–10471.
18. Elenes S, Auerbach A (2002) Desensitization of diliganded mouse muscle nicotinic acetylcholine receptor channels. *J Physiol* 541:367–383.
19. Purohit P, Auerbach A (2007) Acetylcholine receptor gating at extracellular transmembrane domain interface: the "Pre-M1" linker. *J Gen Physiol* 130:559–568.
20. Brønsted JN, Pedersen K (1924) The catalytic decomposition of nitramide and its physicochemical applications. *Z Phys Chem* 108:185–235.
21. Auerbach A (2005) Gating of acetylcholine receptor channels: Brownian motion across a broad transition state. *Proc Natl Acad Sci USA* 102:1408–1412.
22. Bafna PA, Purohit PG, Auerbach AL (2008) Gating at the mouth of the acetylcholine receptor channel: Energetic consequences of mutations in the αM2-cap *PLoS ONE*, 3:e2515.

23. Grosman C, Zhou M, Auerbach A (2000) Mapping the conformational wave of acetylcholine receptor channel gating. *Nature* 403:773–776.
24. Mitra A, Tascione R, Auerbach A, Licht S (2005) Plasticity of acetylcholine receptor gating motions via rate–energy relationships. *Biophys J* 89:3071–3078.
25. Colquhoun D (2005) From shut to open: What can we learn from linear free-energy relationships? *Biophys J* 89:3673–3675.
26. Zhou Y, Pearson JE, Auerbach A (2005) Φ value analysis of a linear, sequential reaction mechanism: Theory and application to ion channel gating. *Biophys J* 89:3680–3685.
27. Jencks WP (1985) A primer for the Bema Hapothle: An empirical approach to the characterization of changing transition state structures. *Chem Rev* 85:511–527.
28. Akk G (2001) Aromatics at the murine nicotinic receptor agonist binding site: Mutational analysis of the αY93 and αW149 residues. *J Physiol* 535:729–740.
29. Zhong W, *et al.* (1998) From ab initio quantum mechanics to molecular neurobiology: A cation π-binding site in the nicotinic receptor. *Proc Natl Acad Sci USA* 95:12088–12093.
30. Katz B, Miledi R (1977) Transmitter leakage from motor nerve endings. *Proc R Soc London Ser B* 196:59–72.
31. Heidmann T, Changeux JP (1980) Interaction of a fluorescent agonist with the membrane-bound acetylcholine receptor from *Torpedo marmorata* in the millisecond time range: Resolution of an ''intermediate'' conformational transition and evidence for positive cooperative effects. *Biochem Biophys Res Commun* 97:889–896.
32. Grosman C, Auerbach A (2001) The dissociation of acetylcholine from open nicotinic receptor channels. *Proc Natl Acad Sci USA* 98:14102–14107.
33. Akk G, Auerbach A (1999) Activation of muscle nicotinic acetylcholine receptor channels by nicotinic and muscarinic agonists. *Br J Pharmacol* 128:1467–1476.
34. Chakrapani S, Bailey TD, Auerbach A (2004) Gating dynamics of the acetylcholine receptor extracellular domain. *J Gen Physiol* 123:341–356.
35. Jin R, *et al.* (2003) Structural basis for partial agonist action at ionotropic glutamate receptors. *Nat Neurosci* 6:803–810.
36. Jha A, Cadugan DJ, Purohit P, Auerbach A (2007) Acetylcholine receptor gating at extracellular transmembrane domain interface: The Cys-loop and M2 M3 linker. *J Gen Physiol* 130:547–558.
37. Qin F (2004) Restoration of single-channel currents using the segmental *k*-means method based on hidden Markov modeling. *Biophys J* 86:1488–1501.
38. Qin F, Auerbach A, Sachs F (1997) Maximum likelihood estimation of aggregated Markov processes. *Proc Biol Sci* 264:375–383.